Available online at www.sciencedirect.com
ScienceDirect
Journal of Sound and Vibration 305 (2007) 534–542
JOURNAL OF SOUND AND VIBRATION
www.elsevier.com/locate/jsvi

Short Communication

Estimation of dynamic structural displacements using fiber Bragg grating strain sensors

Lae-Hyong Kang, Dae-Kwan Kim, Jae-Hung Han*

Department of Aerospace Engineering, Korea Advanced Institute of Science and Technology, 373-1 Guseong-dong, Yuseong-gu, Daejeon, 305-701, Republic of Korea

Received 2 November 2006; received in revised form 1 April 2007; accepted 8 April 2007
Available online 18 June 2007

Abstract

This study investigates dynamic structural displacements estimation using displacement–strain relationship and measured strain data. Strain signals are obtained from fiber Bragg grating (FBG) sensors that have an excellent multiplexing ability. Vibration experiments were performed with aluminum and acryl beam specimens. The beam structures were subjected to various loading conditions, and deformed shapes were reconstructed by using strain signals. The estimated displacements show good agreements with those measured directly from laser displacement sensors. In present study, it is confirmed structural displacements can be estimated using strain data without displacement measurement.

1. Introduction

In order to measure structural shape and deformation, displacement measurement sensor must be installed somewhere. However, sometimes we cannot directly measure displacements of the structure due to the operating conditions. Some examples are the measurements of airplane wing deflection, blade shape changes of windmill or helicopters, tool-tip displacement of line boring machines, etc. In these cases, it is helpful to use attached sensors such as strain gages or fiber optic sensors to measure in-plane strains of the structures.

Many researchers have investigated how to estimate out-of-plane displacements by measuring in-plane strains. Haugse et al. [1,2] suggested the concept of a modal transformation algorithm to recover deformations from strains. They showed the effectiveness of the method by performing an experiment using a cantilevered plate of which modal characteristics were obtained from modal testing in the laboratory. Strains were then measured by the use of strain gages and deformation patterns were predicted. Pisoni and Santolini [3] presented a similar procedure for the determination of displacements at any given point in a vibrating body by using two strain gages. To verify the method, a clamped-end beam was instrumented and experimented upon under different loading conditions. Li and Ulsoy [4] presented a method to measure tool-tip displacement of precision line boring machine. Their method is based on the fact that the vibration displacement can be expressed in terms of an infinite number of vibration modes and be related to the measured strains through the

*Corresponding author. Tel.: +82 42 869 3723; fax: +82 42 869 3710.
E-mail address: jaehunghan@kaist.ac.kr (J.-H. Han).

0022-460X/$ - see front matter © 2007 Elsevier Ltd. All rights reserved.
doi:10.1016/j.jsv.2007.04.037

displacement–strain relationship. In Refs. [5,6], vertical deflections of simple beam models were reconstructed using fiber Bragg grating (FBG) sensor signals and relationship between strain and deflection. As a similar application, strains were reconstructed from operational displacements and displacement-to-strain transformation relationship when strain cannot be measured directly [7,8].

Although many relevant works have been accomplished, most of them [1–4] have used conventional strain gages, which need complex wiring in order to measure the strains at several points. Only static deformations have been treated in most previous literature [5,6]. Even the dynamic deflections were estimated in the previous studies [3,4], the deflections of a few interesting points of the structures were obtained.

The objective of this study is to reconstruct the whole deformation and vibration of structures. The use of strain sensors, which are available to measure in-plane strains, is expanded to out-of-plane vibration measurement and shape sensing. To achieve this goal, we adopted modal approach to construct displacement–strain relationship and used FBG strain sensors to measure the strains at several points.

2. FBG sensor

Fiber optic sensors have been considered as a good alternative transducer for many applications recently. They are immune to electromagnetic interference and their sizes are small enough to be embedded into structures without causing any structural defects. Among these sensors, FBG sensors have been increasingly studied for a variety of applications such as health monitoring, vibration measurement, non-destructive testing, and so forth. FBG sensor arrays are easily made by connecting several Bragg gratings written at different wavelengths serially in a line along the length of a single fiber and addressing each sensor individually using wavelength division multiplexing (WDM) technology. FBG sensors are suitable for the present study because strains at several positions can be measured using only a single optical fiber line.

A FBG is composed of periodic changes of the refractive index that are formed by the exposure to an intense UV interference pattern in the core of an optical fiber. If a broadband light is put into the FBG sensor, it reflects the special wavelength component, called the Bragg wavelength. The Bragg condition is expressed as [9]

$$\lambda_B = 2n_e\Lambda, \tag{1}$$

where λ_B is the Bragg wavelength of FBG, n_e is the effective refractive index of the fiber core and Λ is the grating period. The wavelength, which is determined by the Bragg condition, is reflected at the Bragg grating part, and the other wavelengths pass through it. Fig. 1 shows this process. If we make different Bragg wavelengths along a single strand of optical fiber, strain data can be measured at several points.

The Bragg wavelength is a function of the refractive index of the fiber core and the grating period. If the grating is exposed to external perturbation, such as strain and temperature, the Bragg wavelength is changed. By measuring the wavelength change accurately, the physical properties can be measured. The shift of a Bragg

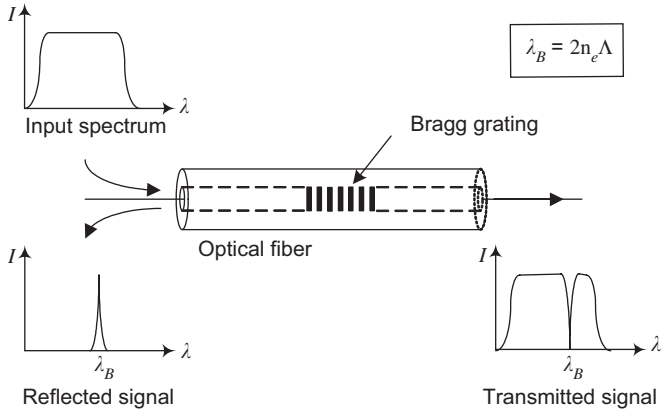

Fig. 1. FBG sensor wavelength-encoding operation.

wavelength due to strain and temperature can be expressed as

$$\Delta\lambda_B = \lambda_B[(\alpha_f + \xi_f)\Delta T + (1 - p_e)\varepsilon], \tag{2}$$

$$p_e = \left(\frac{n_e^2}{2}\right)[p_{12} - v(p_{11} + p_{12})], \tag{3}$$

where α_f is the coefficient of thermal expansion, ξ_f is the thermo-optic coefficient, and p_e is the strain-optic coefficient of an optical fiber. In Eq. (3), v is the Poisson's ratio, and p_{11} and p_{12} are the components of the strain-optic tensor. A germanosilicate glass generally has a strain-optic coefficient of 0.22. Using above equations with the assumption of no temperature change, we can measure the strain from the wavelength shift as

$$\varepsilon = \frac{1}{1 - p_e}\frac{\Delta\lambda_B}{\lambda_B}. \tag{4}$$

3. Displacement–strain transformation relationship

In this study, modal approach is used for construction of displacement–strain relationship. Using displacement mode shapes and strain mode shapes, displacement–strain transformation matrix can be constructed [1]. We assume that displacement and strain of structures can be expressed using finite N mode shapes. Then, the displacement and strain are

$$\{d\} = [\Phi_N]\{\eta_N\}, \tag{5}$$

$$\{s\} = [\Psi_N]\{\eta_N\}, \tag{6}$$

where $\{d\}$, $[\Phi_N]$, $\{s\}$, $[\Psi_N]$ and $\{\eta_n\}$ represent the displacement, the displacement mode shapes, the strain, the strain mode shapes and the modal coordinates, respectively. Each mode shape was obtained using MSC/NASTRAN for the beam model.

From Eq. (6), the modal coordinates can be expressed as

$$\{\eta_N\} = ([\Psi_N]^{\mathrm{T}}[\Psi_N])^{-1}[\Psi_N]^{\mathrm{T}}\{s\}. \tag{7}$$

Substituting Eq. (7) into Eq. (5), we obtain

$$\{d\} = [\Phi_N]([\Psi_N]^{\mathrm{T}}[\Psi_N])^{-1}[\Psi_N]^{\mathrm{T}}\{s\}. \tag{8}$$

According to Eq. (8), it is possible to estimate displacement by the multiplication of strain data by displacement–strain relationship matrix. The rank of $([\Psi_N]^{\mathrm{T}}[\Psi_N])^{-1}[\Psi_N]^{\mathrm{T}}$ cannot exceed the number of used strain sensors. It means we can use as many mode shapes as the number of used sensors at most. Therefore, we must use more sensors if we want to estimate the vibration or deformed shapes accurately at the higher frequency excitation.

4. Experimental results

A schematic diagram of the whole experimental setup is shown in Fig. 2. In this paper, the aluminum and acryl beam structures were considered to estimate the whole deformations of the structures. One end of the beam is clamped and the other end is free. The clamped end is connected to the shaker, which makes the beam vibrate.

IS7000 [10], which is FBG interrogation system of FIBERPRO Inc., was used for the strain measurements. It has modular structure-main frame, laser module, and sensor modules. The laser module is based on the patented wavelength swept fiber laser [11]. It can be easily used to get multipoint strains and the wavelength resolution is 2 pm, but it has a limitation of maximum sampling frequency of 200 Hz.

An aluminum beam specimen with small thickness was fabricated first so that the natural frequencies of the first a few modes are low enough compared with the sampling frequency of IS7000. The dimensions of the

aluminum beam structure is $300 \times 25 \times 0.49\,\text{mm}^3$ (Table 1). Due to small difference between the sensor diameter (0.25 mm) and the thickness of the aluminum beam, the measured strains were overestimated. For this reason, we introduced a compensation factor, which converts the measured strain into the strain on the

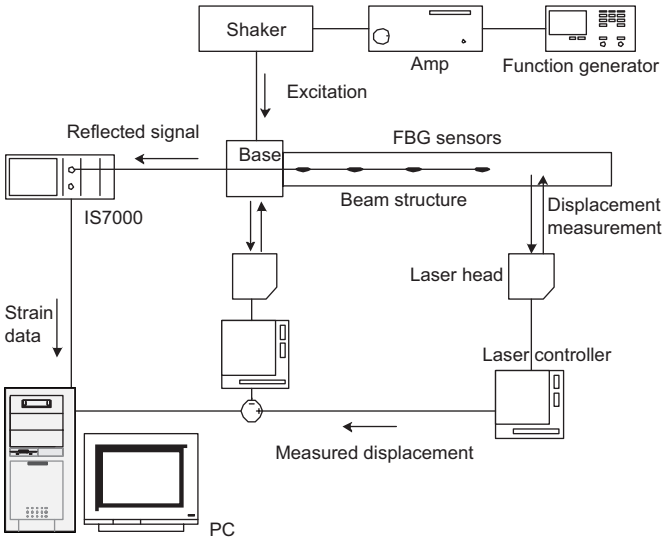

Fig. 2. Schematic of the whole experimental setup.

Table 1
Properties of the beam structures

Property	Aluminum beam	Acryl beam
Length (L) (m)	0.3	0.8
Width (b) (m)	0.025	0.04
Thickness (h) (m)	0.00049	0.01
Young's modulus (E) (Pa)	7.1×10^{10}	3.9×10^{9}
Density (ρ) (kg/m^3)	2710	1160

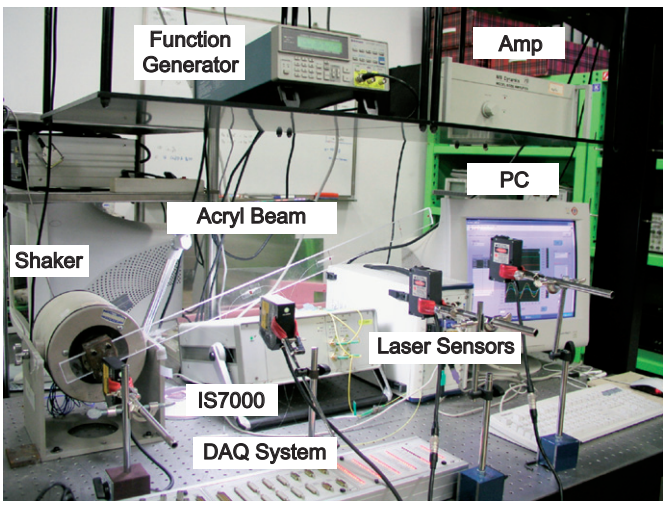

Fig. 3. Photograph of the experimental setup.

Table 2
Natural frequencies of the beam model

Mode no.	Natural frequency (Hz)			
	Aluminum beam		Acryl beam	
	Experiment	Analysis	Experiment	Analysis
1	4.50	4.47	4.43	4.63
2	28.02	28.04	29.59	29.00
3	78.71	78.51	84.24	81.21
4	154.4	153.9	168.4	159.1

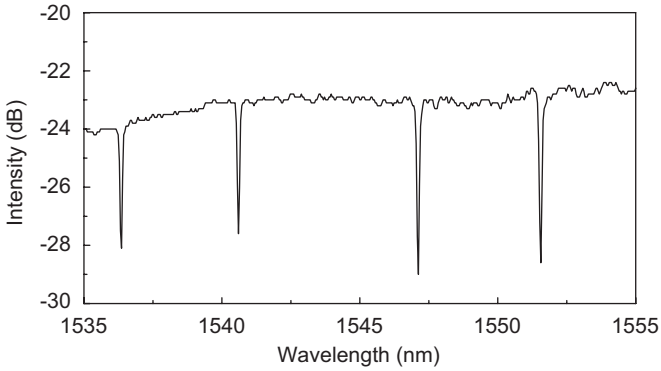

Fig. 4. Transmitted signal of the fabricated FBG sensors.

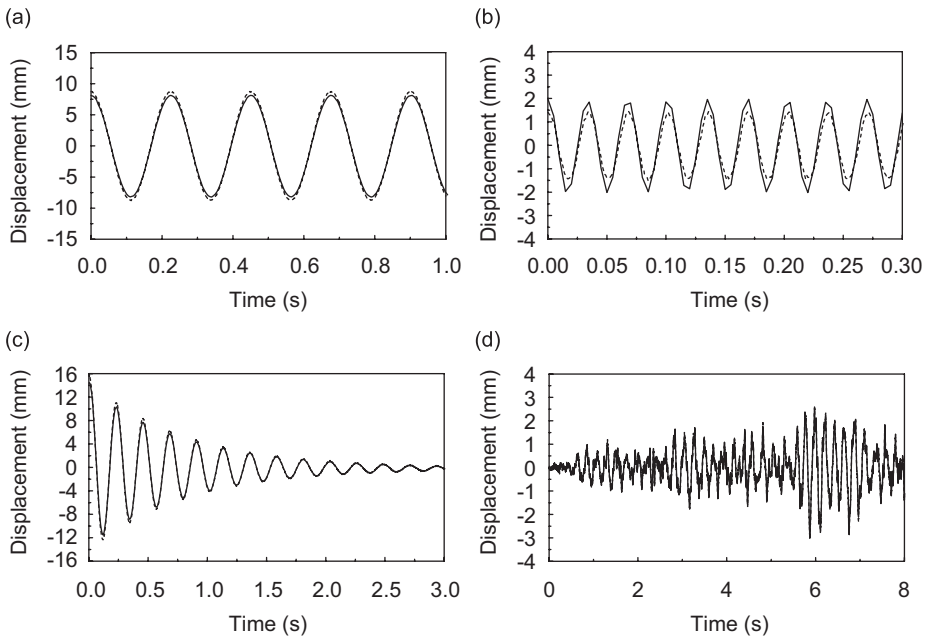

Fig. 5. Displacement measurement results at 700 mm (Acryl beam): (a) first natural frequency excitation, (b) second natural frequency excitation, (c) free vibration, (d) random vibration, ———, estimated displacement; – – – – measured displacement.

surface of the aluminum beam. Then, Eq. (8) becomes

$$\{d\} = [\Phi_N]([\Psi_N]^{\mathrm{T}}[\Psi_N])^{-1}[\Psi_N]^{\mathrm{T}}(\alpha\{s\}), \tag{9}$$

where α is the compensation factor having the value of 0.6622, a ratio of 0.245 mm (half thickness of the beam) to 0.37 mm (half thickness of the beam plus radius of the FBG sensor). We also prepared a thick beam specimen made of acryl and we did not have to consider the compensation factor for the optical fiber strain sensors. The dimensions of the acryl beam structure is $800 \times 40 \times 10\,\mathrm{mm}^3$ (Table 1). A photograph of the experimental setup is presented in Fig. 3. Table 1 shows the properties of the beam models and Table 2 shows the natural frequencies of the structures.

4 FBG sensors along a single fiber were fabricated using different phase masks as shown in Fig. 4. The central wavelengths of FBG sensors are 1536.4, 1540.6, 1547.1, and 1551.6 nm, and they are attached at the positions of 30, 37.5, 114, and 184.5 mm from the base of aluminum beam and at the positions of 80, 100, 304, and 492 mm from the base of acryl beam, respectively. These sensor locations were determined in a way that the transformation matrix in Eq. (8) had the minimum condition number [4].

Using the first 4 mode shapes, deformations of the beam structures were estimated. Displacements were also directly measured at 3 points (aluminum beam: 100, 190, and 290 mm from the base, acryl beam: 300, 500, and 700 mm from the base) using laser displacement sensors. The structures were subjected to various loading conditions and dynamic behaviors of the acryl beam structure are shown in Fig. 5. From Fig. 5, we can see the estimated displacement results show good agreements with those measured directly.

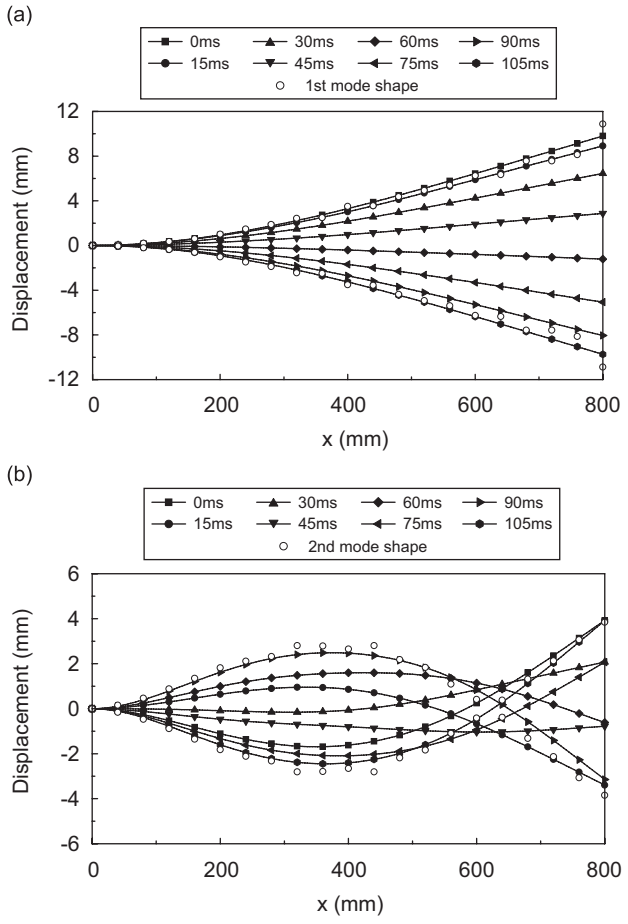

Fig. 6. The estimated deformation of the acryl beam structure: (a) first natural frequency excitation, (b) second natural frequency excitation.

In addition to the local displacement estimation, the estimation results of the whole structural deformation are shown in Fig. 6. Because it is well known that a structure vibrates with the corresponding mode shape if it is excited at its natural frequency, the vibration experiments were performed in the cases of first and second natural frequency excitation for comparison. To obtain experimental mode shapes, we performed a shaker test. We used a modal shaker (for random excitation up to 100 Hz, MB Dynamics MODAL50), a force transducer (PCB Piezotronics 208B02), a laser Doppler vibrometer (LDV, Polytec OFV303), some amplifiers and FFT analyzer (HP3565). The excitation point was fixed and velocities at various locations (each 40 mm from the clamped end) were measured. A Hanning window was utilized for the frequency analysis and STAR MODAL S/W was used to extract modal parameters. The experimental setup is shown in Fig. 7. In Fig. 6, we can see that the deformed shapes of the structures are similar with their own mode shapes, which were obtained by experiment. In acryl beam case, especially at the second natural frequency excitation, we can see the beam vibrates as a complex mode shape due to the large damping effect. In order to measure relative errors

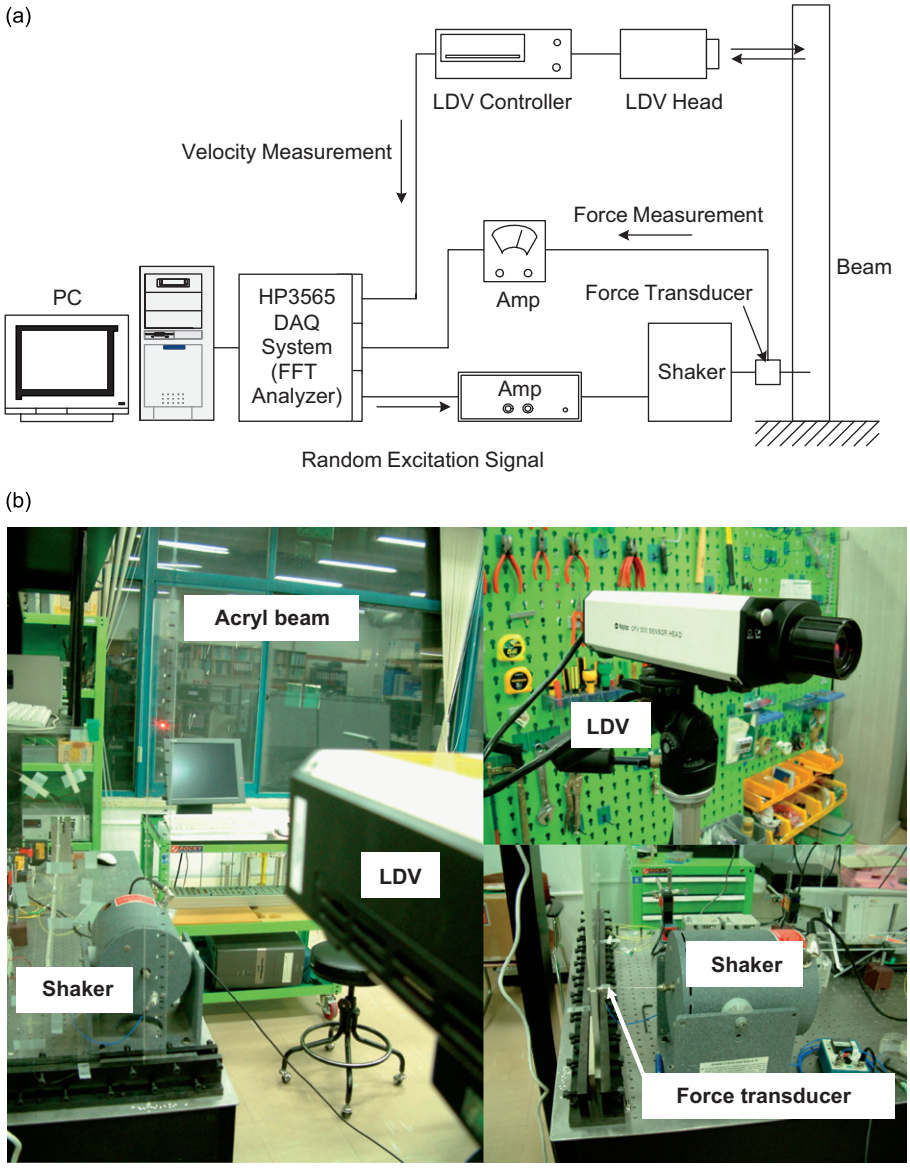

Fig. 7. The experimental setup for modal testing: (a) schematic diagram of the test setup and (b) photograph of the test setup.

Table 3
RMS errors(%) for different loading conditions (aluminum beam)

Measured point (mm)	Excitation					
	3 Hz	First mode (4.5 Hz)	15 Hz	Second mode (28 Hz)	Free	Random
100	9.42	10.2	34.7	8.12	1.64	5.73
190	3.97	4.10	9.12	7.08	1.90	8.00
290	3.99	3.82	6.34	11.91	1.08	7.46

Table 4
RMS errors (%) for different loading conditions (acryl beam)

Measured point (mm)	Excitation					
	3 Hz	First mode (4.43 Hz)	15 Hz	Second mode (29.59 Hz)	Free	Random
300	7.85	5.16	31.7	7.45	1.59	1.01
500	3.28	1.84	4.97	31.0	1.43	0.806
700	5.16	4.46	5.71	30.0	1.39	0.695

between measured and estimated displacements, following RMS (root mean square) percent error was introduced.

$$\text{RMS error} = \frac{\sqrt{\frac{1}{N}\Sigma_{n=1}^{N}(d_{\text{measured}} - d_{\text{estimated}})^2}}{\max(d_{\text{measured}})} \times 100(\%). \tag{10}$$

In Eq. (10), N is the number of time data, d_{measured} represents the measured displacement at a specific point and $d_{\text{estimated}}$ represents the estimated displacement at the same point. These values were obtained at one interesting point of the structure through time. Tables 3 and 4 show the errors at 3 points of the structures according to the different loading conditions. In the off-resonant cases (especially, 15 Hz excitation), the results are worse than the other cases. Because the amplitude level of the beam at off-resonant excitation is not large enough, small noise can generate big relative errors. The damping coefficient of the acryl beam is generally quite large, so it vibrates in a complex mode. Because we used normal mode shapes to estimate structural deformation, the estimated results of the acryl beam are a little bigger than those of the aluminum beam. Nevertheless, the experimental results generally showed the effectiveness of the present method. Using this method, we can estimate the whole structural shape using small number of strain sensors.

5. Conclusion

In this study, displacement estimation method using strain has been introduced. This method requires relationship between displacement and strain mode shapes. Then, structural vibration can be estimated using the displacement–strain relationship with strain sensor signals. Strains were measured by using FBG optical strain sensor array, which has a good multiplexing ability.

To observe the structural deformation, the vibration experiments were performed for the aluminum and acryl beam specimens attached with 4 FBG strain sensors in the laboratory. The beam structures were subjected to various loading conditions, and deformed shapes were well reconstructed by the use of the displacement–strain transformation relationship. The estimated displacement results show good agreements with those measured directly from laser sensors.

This study enables us to estimate the whole structural deformations as well as local displacements with relatively simple computation. The present method can be widely used for applications of vibration sensing and control for the enhanced safety and reliability of the structures [12,13].

References

[1] G.C. Foss, E.D. Haugse, Using modal test results to develop strain to displacement transformation, *IMAC* 1 (1995) 112–118.
[2] P.B. Bogert, E. Haugse, R.E. Gehrki, Structural shape identification from experimental strains using a modal transformation technique, *44th AIAA/ASME/ASCE/AHS/ASC Structures, Structural Dynamics, and Materials Conference*, 2003.
[3] A.C. Pisoni, C. Santolini, Displacements in vibrating body by strain gauge measurements, *IMAC* 1 (1995) 119–125.
[4] C.-J. Li, A.G. Ulsoy, High-precision measurement of tool-tip displacement using strain gauges in precision flexible line boring, *Mechanical Systems and Signal Processing* 13 (1999) 531–546.
[5] M.A. Davis, A.D. Kersey, J. Sirkis, E.J. Friebele, Shape and vibration mode sensing using a fiber optic Bragg grating array, *Smart Materials and Structures* 5 (6) (1996) 759–765.
[6] N.-S. Kim, N.-S. Cho, Estimating deflection of a simple beam model using fiber optic Bragg-grating sensors, *Experimental Mechanics* 44 (4) (2004) 433–439.
[7] S.-W. Seo, K.-J. Kim, B.-K. Bae, Estimation of operational strains from vibration measurements: an application to lead wires of chips on printed circuit board, *Journal of Sound and Vibration* 210 (5) (1998) 567–579.
[8] N. Okubo, K. Yamaguchi, Prediction of dynamic strain distribution under operation condition by use of modal analysis, *IMAC* 1 (1995) 91–96.
[9] A. Othonos, K. Kalli, *Fiber Bragg Gratings: Fundamentals and Applications in Telecommunications and Sensing*, Artech House, Boston, MA, 1999.
[10] http://www.fiberpro.com/products/pdf/IS7000.pdf.
[11] C.-S. Hong, C.-G. Kim, C.-Y. Ryu, J.-W. Park, US Patent No. 6,640,647, 2003.
[12] D.-H. Kim, J.H. Han, D.H. Kim, I. Lee, Vibration control of structures with interferometric sensor non-linearity, *Smart Materials and Structures* 13 (1) (2004) 92–99.
[13] R.M. Measures, *Structural Monitoring with Fiber Optic Technology*, Academic Press, New York, 2001 (Chapter 2).